American Industrial Hygiene Assoc Journal 30: 257-75 (1969)

726781

To: Dr Snyder
From: Mg Cook

note p 271
Table V

OCT 13 1969

The Effect of Particle Size on the Regional Deposition of Inhaled Aerosols in the Human Respiratory Tract

MORTON LIPPMANN, Ph.D., and ROY E. ALBERT, M.D.

New York University Medical Center, Institute of Environmental Medicine, 550 First Avenue, New York, New York 10016

The effect of particle size on the regional deposition of aerosols inhaled through the mouth was determined in 93 studies on 34 subjects. The test aerosols were spherical monodisperse insoluble iron oxide particles (specific gravity 2.5) containing radioactive tags, ranging in median unit density diameter from 2.1 to 12.5-microns ($\sigma \cong 1.08$). Particles deposited on the bronchial tree were translocated to the stomach by mucociliary clearance which was essentially complete within the first day. The proportion of the initial lung burden of radioactive particles removed during the first 24 hours provided a functional measure of tracheo-bronchial deposition. A portion of the inhaled aerosol was deposited in the head by impaction. As an impactor, the tracheobronchial tree is more efficient. For each individual subject, head and tracheobronchial deposition increased with increasing particle size. Alveolar depositions decreased with size for particles larger than 4-microns.

Introduction

KNOWLEDGE OF THE regional deposition of inhaled particles forms the basis for estimating the quantity of inhaled aerosol which reaches the various parts of the respiratory tract and is therefore one of the essential factors in the characterization of the toxicity of airborne contaminants.

It has been long recognized that the depth of penetration of an inhaled particle into the respiratory tract is a function of its mass (that is, size and density) and of the respiratory flow. However, relatively few studies have attempted to relate these factors to regional deposition. In mouth breathing studies with monodisperse aerosols of triphenyl phosphate in the size range 0.11 to 6.3-microns in diameter, Landahl, *et al.*[1,2] fractionated the exhaled air into four sequential components. The residual airborne particle burdens in each component were presumed to have come from different lung regions. The results obtained were compared to predicted values for the same breathing patterns obtained from Landahl's[3] previous theoretical calculations. The agreement was sufficiently good for the authors to conclude that the theoretical calculation was correct.

Brown *et al.*[4] studied regional deposition during nose breathing, using china clay aerosols in narrow size ranges ($\sigma_g = 1.25$), with count median diameters between 0.9 and 6.5-microns. They collected the exhaled air in seven sequential components and used CO_2 content of each fraction as a tracer to identify the region from which the exhaled air originated. The validity of these data depends on the accuracy of the association between the various exhaled air fractions and their presumed sources. The Brown data have been questioned on the basis that the CO_2 tracer diffuses much more rapidly than the particles.[5] Hence, the measured

This paper is an abridgement of a doctoral thesis by the senior author. This thesis has been accepted by the faculty of the Graduate Division of the School of Engineering and Science of New York University in partial fulfillment of the requirements for the degree of Doctor of Philosophy. This investigation was supported in part by a project grant from the U. S. Public Health Service, Grant UI-00484. It was also aided by a grant from the Americal Medical Association Education and Research Foundation. This work is part of a center program supported by the National Institute of Environmental Health Sciences Grant ES 00260.

REPOSITORY MMES-ORNL
COLLECTION Snyder's Files
BOX No. 2
FOLDER Inhalation

A-00631

Human Studies Project 1185323

CO_2 values in the exhaled air may have differed significantly from the corresponding CO_2 concentration in the alveolar spaces, causing an error in the volume partitioning, and minimizing the alveolar deposition.

Altshuler *et al.*[5] estimated regional deposition from mouth breathing experiments in which measurements of both the concentration of a monodisperse triphenyl phosphate aerosol and the respiratory flow were made continuously during individual breaths. Using a continuous tubular filter bed model as a theoretical analog for the respiratory tract, they calculated regional deposition in the upper and lower tract components for various values of anatomic dead space. The upper tract penetration during inspiration, pause, and expiration was derived from the expired aerosol concentration corrected for aerosol mixing. The particle size for maximum alveolar deposition was estimated to be greater than 2-microns, but its value could not be determined, since only one particle greater than 2-microns was used in the experiments. The data from nose breathing experiments of Brown *et al.*[4] had indicated maximal alveolar deposition at about 1.6-microns.

In this laboratory, we have been involved in an extended series of experiments dealing with the deposition and clearance of insoluble radioactive aerosols in humans and donkeys by a method involving external measurements of the gamma-emitting particles in the head, lung, and abdomen. Since the initial studies on humans over a decade ago, it has been evident that the method could provide an assessment of regional lung deposition because particles deposited on the bronchial tree are cleared by mucociliary action within a relatively few hours, while particles that penetrate into the deeper and nonciliated regions of the lung are removed over a period of months.[6] Radioactivity measurements of the head immediately after inhalation can also provide estimates of the fractional deposition in the nose or mouth, depending on the mode of breathing.

After a method for generating monodisperse insoluble radioactive particles was developed,[7] an initial series of experiments was done on 11 subjects who inhaled 5- or 3-micron iron oxide particles.[8,9] These experiments served to confirm the much earlier observations on the characteristics of bronchial clearance, and also provided preliminary estimates of regional deposition which differed considerably from those reported by other methods. Since then a much larger number of experiments have been completed which have also incorporated additional refinements in the experimental technique.

The purpose of this paper is to present the new experimental data, and also to describe the cumulative results obtained to date with monodisperse aerosols in order to define the relationship of regional deposition to particle size in the 2- to 8-micron particle size range. The experimental findings dealing with the character of bronchial clearance will be described in another paper.

Methods

The methods used for the generation and administration of the radioactive aerosols as well as the measurement of chest activity were comparable in most respects to those described earlier.[6-10] However, as detailed in later sections, the methods differed from the previous study in the following respects: (1) The arrangement of the scintillation detectors was altered in order to obtain measurements of chest activity that were less dependent on the location of particles in the lung; (2) the respiratory flow rates were measured; and (3) many of the studies involved the inhalation in rapid sequence of two aerosols differing in particle size, each aerosol having been tagged with a different isotope.

Generation and Characterization of Test Aerosols

The test aerosol in each inhalation was composed of iron oxide spheres within a narrow size range which were tagged with either ^{198}Au or ^{99m}Tc as a tracer. The aerosols were produced with spinning-disc generators which have previously been described.[7,10] The median diameters of the aerosols varied from 1.3 to 7.9-microns, and the geometric standard deviation averaged 1.08. The technique

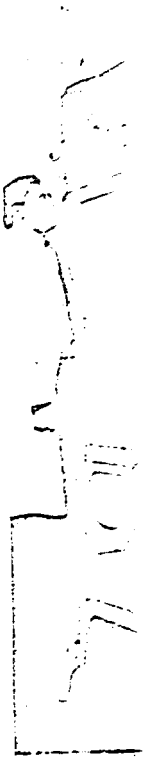

FIGURE 1.
ject is breat
respiratory v
generator h

of using ta
feed for a
insoluble
nonleachin
tags has b

One spi
so that th
applied to
using diffe
different
feed suspe
size and t
ing any o
generator.
described,
haled. In
inhalation
followed
a 1-minu
aerosol wi
unaware

1185324

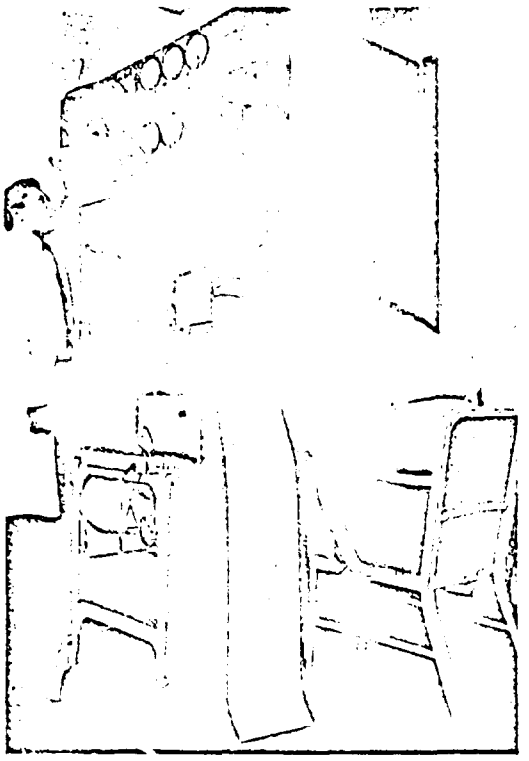

FIGURE 1. Simulated inhalation exposure. Subject is breathing through mouthpiece connected to respiratory valve through side wall of spinning-disc generator hood enclosure.

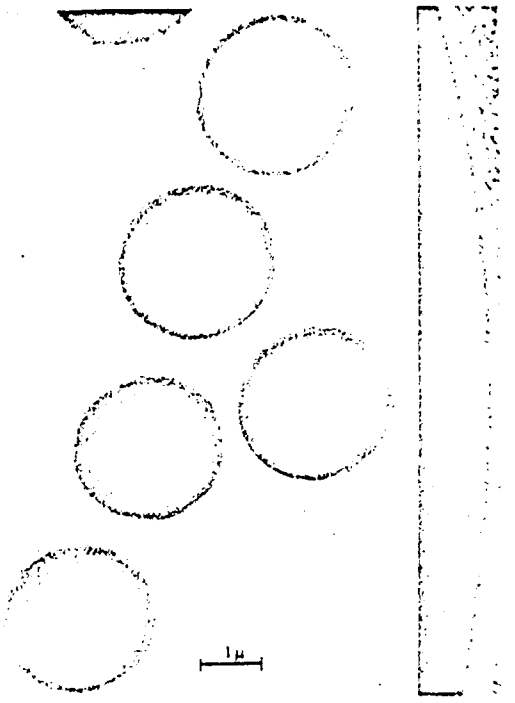

FIGURE 2. Electron micrograph of iron oxide particles from spinning-disc aerosol generator as inhaled by volunteer subjects. An enlarged view of the edge of one particle is shown at the right.

of using tagged colloid suspensions as a liquid feed for a spinning-disc generator to produce insoluble monodisperse spheres containing nonleaching gamma-emitting radioisotope tags has been described.[7]

One spinning-disc generator[10] was set up so that three different liquid feeds could be applied to the disc in rapid succession. By using different iron oxide concentrations and different radioisotope tags in the different feed suspensions, aerosols of different particle size and tag can be produced without changing any of the operating parameters of the generator. In thirty of the test runs to be described, two different aerosols were inhaled. In the most of these, a 1-minute inhalation of a smaller-sized aerosol was followed after a 10- to 15-second pause by a 1-minute inhalation of a second, larger aerosol with a different tag. The subject was unaware of the timing of the beginning and end of the aerosol generation interval and was concentrating on producing a uniform breathing pattern throughout the entire period. Thus, the two successive inhalations at similar breathing conditions simulate a simultaneous exposure, at least in terms of the subsequent particle clearance.

Figure 1 shows a simulated inhalation exposure. The subject inhales test aerosol from the generator through a respiratory valve connected within the hood enclosure to the output duct.

The particle size distribution for each test run was analyzed by sizing a representative sample collected on a 25-mm-diameter disc of membrane filter (Millipore, Type AA). A minimum of 50 particles per sample were sized, using a 90× apochromatic oil immersion objective and a filar micrometer eyepiece. Under the light microscope, the particles appeared to be solid spheres. Actually, they were porous aggregates of smaller colloid spheres. The edges of the particles have

1185325

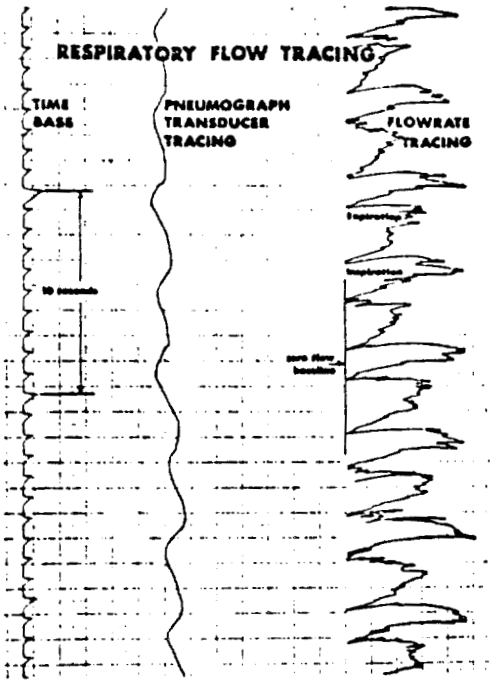

FIGURE 3. Respiratory flow tracing.

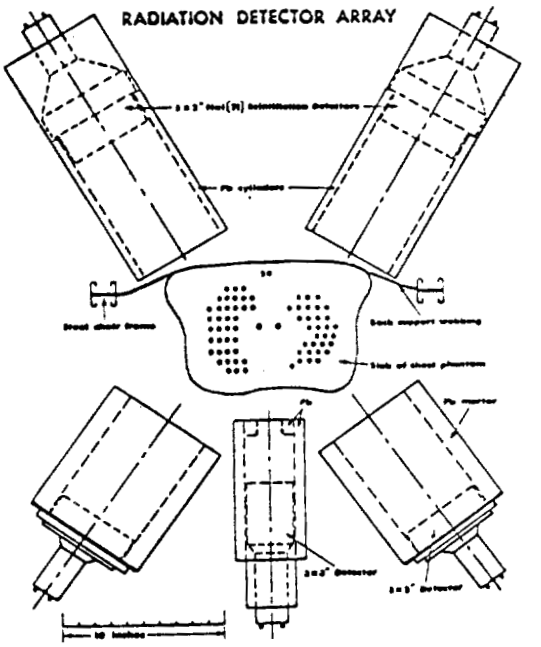

FIGURE 4. Positions of radiation detectors within cylindrical collimators relative to chest phantom or subject.

a very slight surface irregularity which can be seen in the magnified view of the particle edge at the right side of Figure 2. As reported previously, measurements with a Timbrell aerosol spectrometer demonstrated that the density of the particles was 2.5 compared to the parent material density of 4.0 for iron oxide.[10]

Control and Measurement of Respiratory Variables

The subject regulated his breathing pattern to conform to audible and visible signals. A breathing frequency of 14 respirations per minute was maintained constant in all runs. A solenoid-actuated three-way 1-inch ball valve controlled by an electrical timer separated the inhaled and exhaled air, permitting the subject to inhale particles from the output duct of the aerosol generator and to direct his exhaled air through a filter canister and dry gas meter. The subject's inspiratory and expiratory flow rate was measured with a small heated film anemometer sensor (Thermo-Systems, Inc., 2500 Cleveland Ave. N., St. Paul, Minnesota 55113) located in the common port of the respiratory valve (that is, between the rotating ball of the valve and the mouthpiece). The panel meter of the power unit controlling the sensor was visible to the subject during the run, permitting him to control his inspiratory flow rate at approximately the desired level. The flow transducer output signal was a voltage linearly proportional to the air velocity in the breathing port. It was fed to a continuous chart recorder to provide a permanent record. A sample tracing is shown in Figure 3. The total inhaled volume was measured by integrating the flow rate tracings planimetrically, and also by measuring the total exhaled volume passing through a dry gas meter. The peak inspiratory flow rates were measured on the flow rate tracing.

Detection of Radioactivity Burdens

All measurements were carried out with the subject in a low-radiation-background chamber having 6-inch-thick steel walls. As shown schematically in Figure 4, the particle

1185326

retention was measured by a ring of four 5-inch-diameter by 2-inch NaI(Tl) scintillation detectors whose faces were approximately 16 inches from the center of the chest cavity. The detectors were shielded by cylindrical lead-filled collimators extending from the crystals to the vicinity of the chest wall in order to restrict the field of measurement to the chest.

The four 5-inch by 2-inch collimated scintillation detectors were aligned on a common plane and were supported by mounting brackets attached to the steel frame of a chair which also supported the subject (see Figure 7). The subject's height relative to the detectors was adjusted by means of a seat-jacking mechanism mounted at the back of the chair to bring the axis of the detectors to one-third the distance down from the supersternal notch to the xyphoid. A ¾-inch-diameter spot of light cast on the subject's neck by a miniature spotlight mounted between and above the front detectors permitted reproducible positioning of the subject. By means of a mirror mounted on the chair, the subject was able to continually check his position against the light circle. One of the ring detectors and the smaller tracheal detector (to be described) were mounted on a rotating arm, which could be swung clear, permitting the subject free access to the chair. The rotating arm was always returned to the same position with the aid of built-in position markers on the rotating arm.

With the above configuration, the total count received by the four detectors is relatively independent of the distribution of the radiation sources within the lung as determined by measurement of point sources in a Masonite phantom.[11] The degree of uniformity in counting efficiency is illustrated in Figure 5. The average counting efficiency for activity in the major bronchi and trachea is about 13% higher than the average sensitivity for the lung as a whole, which was 17 cpm/nCi for both ^{198}Au and ^{99m}Tc.

The contribution of swallowed particles to lung activity measurements was determined in experiments in which radioactive particles suspended in distilled water were swallowed by three of the inhalation subjects. The lung

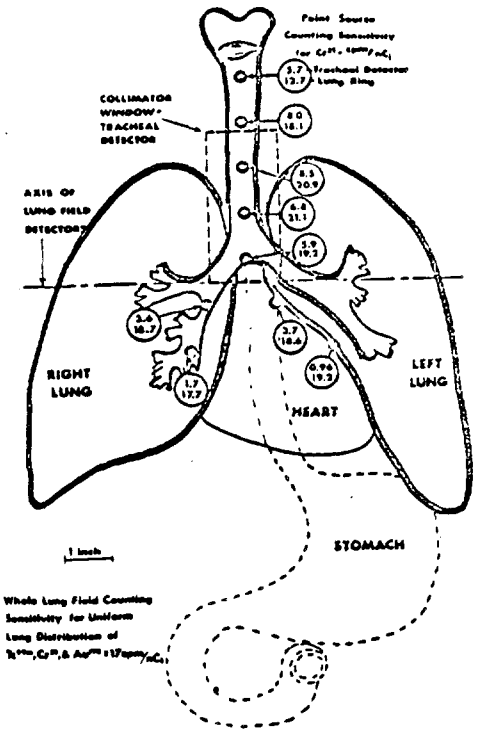

FIGURE 5. Approximate positions of trachea, lungs, heart, and stomach, with lung counting sensitivities at indicated positions.

field counts due to the material in the stomach remained at about 10% of that which uniform lung deposit would have caused for periods ranging from about 20 to 40 minutes. Within the next half-hour, the lung field count dropped off to near background.

In addition to the ring of 5-inch detectors, a 3-inch by 3-inch NaI(Tl) scintillation detector was positioned over the front of the chest to provide a measurement field largely restricted to the trachea and adjacent tissue. This detector was housed in a cylindrical lead collimator which had an aperture in the form of a vertical slit 1.5 inches wide by 3.5 inches high. Its axis was 1.5 inches above the height of the axis of the radial detectors, and its face was recessed 4¼ inches into the collimator, approximately 10 inches from the center of the chest. The sensitivity of the tracheal detector for point sources at various positions within the lung phantom is also illustrated in Figure 5.

1185327

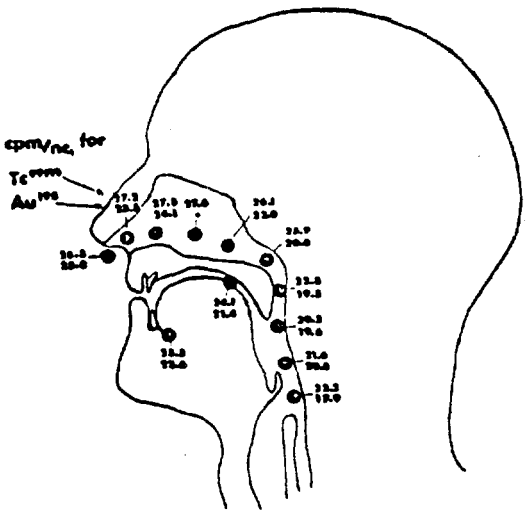

FIGURE 6. Counting sensitivity for sources within head at indicated positions.

The retention of particles deposited within the head was measured with the same ring of 5-inch scintillation detectors used for measuring the chest retention. The subject moved from the chest to the head counting position by shifting the unattached cushioned seat from the normal upper seat support to a second seat support which was 8 inches lower. As shown in Figure 6, a uniform sensitivity within about ± 15% was obtained for head burdens measured with this array.

The head field ring detector sensitivities were determined for ^{99m}Tc and ^{198}Au by positioning a point source within the tip of a catheter tube at various positions within the head of one of the inhalation subjects.

With the subject in a standing position, anterior and posterior measurements of the abdomen were made with a single 8-inch by 4-inch detector at a distance of 14 inches from the surface of the body. Chest radioactivity was screened from view of the detector by use of a 1-inch-thick vertical shield which covered the lower half of the head and the entire chest down to a level 3 inches below the xyphoid. The axis of the detector was 7 inches below the xyphoid.

The experiments in which a known amount of radioactive particles was swallowed by three of the subjects, [redacted], [redacted], and [redacted] provided the calibration factors. Serial measurements on each subject indicated that the average of the anterior and posterior abdominal measurements throughout the first day remained constant within ± 15% except for a brief (~ 1 hour) interval during which the abdominal count dropped to about half of the average level of the first few hours. The average counting sensitivity in the abdomen was ~20% lower for subject [redacted] than for subject [redacted], with subject [redacted] in between.

In the most recent inhalation experiments, additional measurements were made of the activity within the stomach, using a 3-inch by 3-inch NaI (Tl) detector within a 3½-inch i.d. cylindrical collimator. The face of the detector was recessed 3¼ inches into the collimator, whose face was ½ inch behind the webbing of the chair on the left side. The axis of the detector was 8 inches below the axes of the 5-inch detectors and in line with the expected location of the stomach.

The output signals from the scintillation detectors were processed by a 400-channel pulse height analyzer which could be operated as four 100-channel analyzers. Thus, four different measurements could be made simultaneously. In some of the experiments, the four 5-inch detectors' signals were combined into one 100-channel band, while in others they were separated into left-side and right-side pairs. The trachea, stomach, and abdominal detectors were each analyzed in 100-channel bands. The analyzer was calibrated at 5 keV per channel, giving a total energy range of 0 to 500 keV. The isotopes used were ^{198}Au with a half-life of 2.7 days and a gamma photopeak energy of 411 keV, and ^{99m}Tc with a half-life of 6.0 hours and a gamma photopeak energy of 140 keV. Photopeak counts in the energy band 372.5 to 477.5 keV (channels 75 to 95) were summed to provide a measure of gold tag in the chest. For ^{99m}Tc, the energy band from 122.5 to 162.5 keV (channels 25 to 32) was used.

For runs involving the inhalation of two particle distributions, the larger particles tagged with ^{99m}Tc and the smaller ones with ^{198}Au, the contribution of activity from the

1185328

higher-energy ^{198}Au appearing in the photopeak region of the lower-energy ^{99m}Tc was determined from the amount of ^{198}Au scatter in an energy band between the photopeak regions of the two isotopes. In the energy region selected (167.5 to 207.5 keV) where there was negligible technetium count, the ^{198}Au scatter was 70% of that in the ^{99m}Tc photopeak region itself.

Experimental Procedure

Most inhalation studies began in midmorning. The subjects were given no special instructions with respect to eating or smoking before the start of the inhalation exposure. Each test inhalation consisted of a brief (usually 1 minute) exposure to a test aerosol composed of monodisperse spherical iron oxide particles containing a very small (<1%) mass fraction of either ^{198}Au in metallic form or $^{99m}Tc_2S_7$. In most of the test inhalations starting with H-27, a second 1-minute inhalation was begun about 10 seconds after the end of the first. In these double exposures, the first exposure involved a smaller-size particle with ^{198}Au tag ($T_{\frac{1}{2}}$ = 2.7 days), while the second exposure involved a larger iron oxide particle with ^{99m}Tc tag ($T_{\frac{1}{2}}$ = 6.0 hours). The smaller of the two aerosols always exhibited the greater fractional long-term retention; hence the use of the longer half-life isotope (^{198}Au) on the smaller particles. This maximized the length of time that measurable radiation burdens could be followed.

On completion of the inhalation, the subject was directed to the chair in the whole-body counter where the retention measurements were made (Figure 7). In almost every test, the first chest count was started within 1 minute after the end of the inhalation.

Most of the subjects were members of the departmental staff or affiliated institutions. All were volunteers. They were highly motivated, were extremely cooperative, and adapted readily to the experimental protocol requiring that they inhale on signal at an appropriate flow rate and tidal volume.

Results

Forty-five inhalation tests were performed

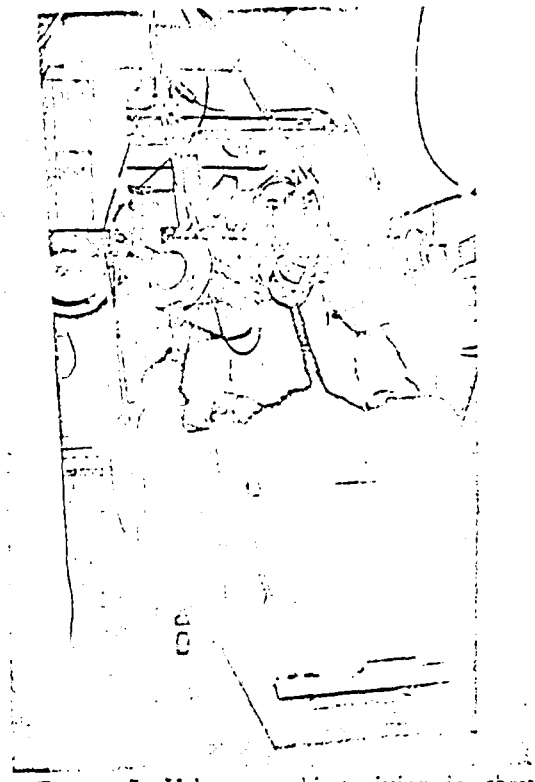

FIGURE 7. Volunteer subject sitting in chest counting position in chair within whole-body counter.

by 26 individual subjects in the current test series. Of these, 32 involved two separate inhalations in rapid succession, so that the total number of test aerosols whose deposition and clearance was studied was 77. In addition, results are summarized for 16 previously reported inhalation exposures to 11 subjects,[8,9] three of whom participated in the current series.

The vital statistics and smoking histories of the subjects are presented in Table I. All but one of the subjects ([redacted]) were males. As shown in the table, they varied considerably in size, age, and smoking history. The only known abnormalities were a pronounced smoker's cough in subject [redacted] and chronic cough in subject [redacted], a 68-year-old nonsmoker with chronic bronchitis.

Seven subjects were exposed to aerosols of four or more different sizes. The overall lung retentions as a function of time past exposure are shown for four of them in Figure 8. In each of the panels in this figure, the clear-

1185329

TABLE I
Vital Statistics of Inhalation Subjects

Subject	Age (years)	Height (inches)	Weight (pounds)	Current Smoking History
[redacted]	46	70	185	Ex-smoker for 9 years, 1½ pkg./day 15 years
	34	64	125	20 cig./day (filter) 16 years
	42	73	195	Cigar and pipe 21 years
	32	71	165	Nonsmoker
	28	73	147	35 cig./day, (filter) 5 years
	30	74	165	Nonsmoker
	53	75	250	40 cig./day (filter) 20 years
	68	70	180	Nonsmoker
	21	68	170	Nonsmoker
	48	70.5	155	30 cig./day (filter) 20 years
	33	66	145	30 cig./day (no filter) 12 years
	29	72	175	20-30 cig./day (no filter) 15 years
	28	68.5	158	20 cig./day (filter) 8 years
	30	65	200	20 cig./day (no filter) 10 years cigar and pipe only 3 years
	30	69	155	25 cig./day (no filter) 17 years
	36	70	180	30 cig./day (no filter) 10 years
	43	74	192	Ex-smoker for 10 years, 40 cig./day 15 years
	21	74	190	Nonsmoker
	36	79	220	20 cig./day (no filter) 15 years
	34	70	175	Nonsmoker
	73	66	185	Cigar and pipe 45 years
	46	71	185	40 cig./day (filter) 20 years
	42	74	200	Occasional cigarette smoker
	38	70	144	5 cig./day, 10 pipes/day 8 years
	25	69	167	30-40 cig./day (filter) 5 years
	33	70	190	Nonsmoker
	26	74	180	Nonsmoker
	24	62	126	Ex-smoker 4 years, 7 cig./day 6 years
	26	74	210	30 cig./day (filter) 7 years
	67	72	200	Ex-smoker 12 years, 20 cig./day (no filter) 30 years
	30	70	248	Nonsmoker
	42	74	195	Nonsmoker
	29	73	184	Nonsmoker
	24	71	185	25 cig./day (filter) 6 years

[a] Chronic bronchitis.
[b] Uranium miner.
[c] Female.

TABLE II
Lung Clearance after First Day

Subject	Test	First Day Clearance Cum. (%)	Second Day Clearance Cum. (%)	First Week Clearance	
				ΔT Days	Cum. (%)
[redacted]	H-21	80	80	—	—
	H-27A	40	48	3	57
	H-28A	50	50	—	—
	H-30A	81	85	—	—
	H-33A	40	40 (3 day)	8	54
	H-35A	77	77	4	82
	H-36	46	—	6	47
	H-37	23	27 (4 day)	7	35
	H-49A	52	—	8	52
	H-1	45	50	6	56[a]
	H-2	28	—	4	38
	H-4	54	54	—	—
	H-7	65	70	—	—
	H-8	60	63	4	66
	H-11	85	85	—	—
	H-58A	78	—	6	80
	H-65A	69	71	—	—

[a] Last reading at 56 days—85% clearance.

1185330

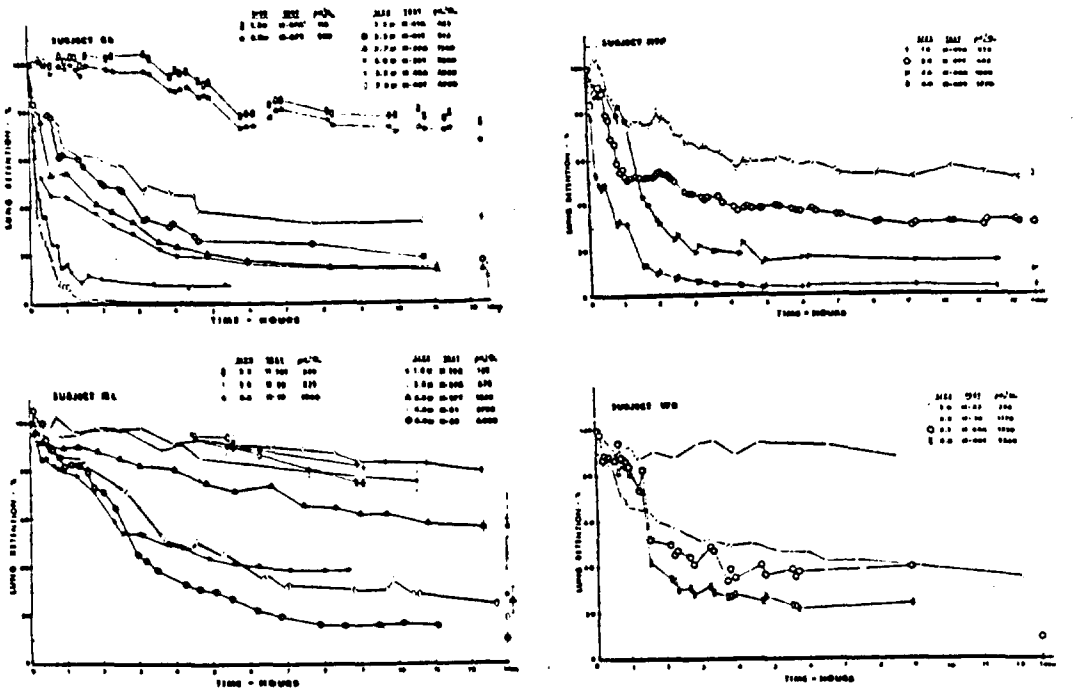

FIGURE 8. Lung retention versus time at various particle sizes for four inhalation subjects. Uncertainties due to counting statistics are indicated by vertical bars for those points where they are greater than the size of the symbol.

ance curves were identified as to test number, mass median particle diameter (d_m) in microns, and the product $\rho d^2{}_m Q_n$, where ρ is the particle density in grams per cubic centimeter, and Q_n is the average inspiratory flow rate in liters per minute.

Figure 8 demonstrates that the patterns of clearance during the first 12 hours varied widely from subject to subject. For the purpose of the characterization of regional deposition, the kinetics of the bronchial clearance process have been ignored, since it was sufficient to measure the net effect of the clearance processes taking place during the first day, and to verify that clearance taking place during the first day was bronchial clearance. The data in Table II indicate that, for the group of subjects tested, the rate of clearance after the first day was very much slower than that within the first day postexposure.

The depositions within the major functional regions of the respiratory tract in the experimental mouth breathing inhalation tests are summarized in Table III. The regions are (1) the mouth, (2) the pharynx–larynx (P-L), (3) the ciliated tracheobronchial tree (T-B), and (4) the nonciliated alveolar spaces (Alv.).

Mouth deposit has been defined as that part of the head deposition recoverable within the first few minutes postinhalation by gargling and mouthwashing. The residual head deposition is designated the pharyngeal and laryngeal (P-L) component. The data indicate that the major fraction of the head deposition in the current test series took place beyond the oral cavity in all but one subject ([redacted]). Most subjects deposited between about 15% and 40% of the head deposit in the mouth, while one subject ([redacted]) averaged only about 5% in four tests.

The abdominal measurements made approximately 1 hour after the inhalation provided estimates of the quantity of head and lung deposit which was cleared and swallowed. Table IV shows a comparison of the estimated abdominal burdens and the head and chest activity cleared via the esophagus

1185331

TABLE III
Test Inhalation Data Summary—Mouth Breathing

Subject	Test	Particle Size, d_m (σ_g)	Min. Volume (liters)	Inspiratory Flow (lpm) Q_p[a]	Q_e[b]	$\rho d^2 = Q_e$	Regional Deposition % of Inhaled Aerosol: Mouth	P-L[c]	T-B[d]	Alv.[e]	Exhaled Aerosol (%)	Lung Clearance (%) 10 hr	24 hr
	H-65A	3.02(1.08)	10.8	53.3	22.8	520	0.7	46.8	29.9	13.5	9.1	68	69
	H-65T	5.33(1.07)	8.7	44.4	18.4	1307	14.7	51.6	21.7	3.0	8.9	80	88
	H-18	4.45(1.11)	7.1	34.6	14.2	703	—	—	21.8	19.4	—	50	53
	H-22	4.65(1.12)	21.5	58.0	35.6	1930	→	(38.5)†	32.2	26.4	3.3	45	55
	H-23	4.77(1.12)	16.2	88.0	61.3	3480	→	(47.4)†	37.9	3.3	11.4	85	92
	H-1	3.56(1.21)	19.0	—	—	1220*	8.0	5.0	29.9	44.8	12.0	42	40
	H-2	3.43(1.12)	9.8	—	—	570*	2.8	2.2	22.9	59.0	12.5	26	22
	H-8	5.03(1.10)	15.1	—	—	2200*	21.6	43.4	18.5	12.4	3.8	60	60
	H-32A	3.68(1.08)	17.5	75.1	36.7	1240	15.6	32.2	41.7	6.2	4.3	85	87
	H-32T	4.96(1.06)	16.2	66.9	33.9	2080	23.9	28.7	34.3	3.8	9.3	85	90
	H-41A	2.46(1.07)	15.2	60.4	30.2	455	1.1	—	45.4	23.4	—	66	66
	H-41T	3.16(1.08)	17.0	55.6	32.5	813	2.8	—	60.7	12.5	—	80	83
	H-48A	5.76(1.05)	16.1	67.5	36.5	3080	16.5	54.7	≥24.2	≤1.8	2.8	~95	—
	H-48T	7.25(1.06)	17.3	64.6	36.3	4780	28.7	46.0	≥23.0	≤1.0	1.3	~99.5	—
	H-67A	1.34(1.08)	11.1	49.8	25.7	115	1.5	8.9	19.9	51.0	18.6	22	28
	H-67T	2.04(1.12)	10.0	44.1	22.1	230	1.1	11.0	22.3	43.2	22.4	28	34
	H-59A	3.90(1.10)	19.1	59.5	34.4	1310	1.8	27.2	60.1	3.2	7.8	94	95
	H-59T	5.04(1.11)	19.1	58.8	35.5	2250	2.3	38.9	51.7	2.7	4.5	84	95
	H-58A	3.94(1.16)	15.7	55.7	28.1	1090	4.2	36.9	42.3	11.9	4.7	78	78
	H-58T	5.19(1.11)	16.2	60.7	26.6	1790	10.9	34.0	48.8	4.2	2.1	92	92
	H-26	3.77(1.17)	14.1	64.2	32.8	1170	→	(39.4)†	46.6	11.7	2.3	60	80
	H-33	2.59(1.05)	6.3	48.6	20.2	338	2.9	15.1	21.2	31.7	29.1	15	40
	H-44A	5.14(1.07)	12.7	53.9	23.6	1550	21.2	47.4	25.8	2.5	3.1	60	91
	H-44T	6.80(1.06)	13.3	53.2	22.2	2560	29.0	52.4	≥16.3	≤0.2	2.1	76	≥99
	H-5	5.00(1.12)	12.0	—	—	1490*	20.0	10.0	64.2	2.0	4.2	65	95
	H-13	5.10(1.14)	16.3	—	—	2120*	45.0	15.4	32.2	5.3	2.1	67	86
	H-30	3.68(1.09)	21.0	74.0	40.4	1360	1.8	11.9	44.2	11.8	30.3	69	79
	H-35A	3.90(1.09)	17.0	82.2	38.5	1460	17.7	46.5	18.7	9.2	7.9	62	67
	H-35T	5.19(1.07)	20.3	92.4	39.5	2650	56.3	5.4	25.3	6.3	6.7	80	80
	H-57A	4.05(1.13)	15.2	81.0	28.0	1150	→	(68.5)†	12.5	12.5	6.5	50	50
	H-57T	5.33(1.11)	16.0	89.2	32.2	2290	→	(84.5)†	14.8	—	0.7	84	100
	H-45A	3.41(1.08)	20.4	91.0	41.7	1210	11.8	20.3	44.3	19.0	4.6	54	70
	H-45T	4.65(1.07)	26.2	88.5	45.6	2460	12.1	21.1	54.5	4.7	2.6	69	92
	H-46A	3.41(1.08)	19.7	72.8	42.8	1240	10.7	30.2	42.3	9.3	7.5	79	82
	H-46T	~4.7	22.1	73.3	43.4	~1700	13.3	39.5	35.9	4.9	6.4	84	88
	H-63A	4.05(1.06)	23.2	63.8	45.5	1870	37.3	39.6	16.3	4.1	2.7	77	80
	H-63T	5.10(1.08)	23.7	75.8	47.7	3150	31.7	44.9	16.0	3.5	3.9	82	82
	H-42A	3.62(1.06)	13.9	51.1	30.8	1010	11.0	—	65.8	7.3	—	82	90
	H-42T	4.98(1.05)	17.2	56.6	34.7	2140	21.3	—	53.0	1.1	—	90	98
	H-43A	3.59(1.07)	21.4	80.7	42.5	1370	9.7	39.6	30.4	13.1	7.2	61	70
	H-43T	4.93(1.06)	23.2	75.5	44.4	2700	13.0	59.1	22.6	2.5	2.8	81	90
	H-53A	3.74(1.14)	15.5	73.3	29.9	1050	7.6	18.6	25.8	30.2	17.8	40	46
	H-53T	5.12(1.09)	17.4	80.5	34.5	2260	13.6	30.0	25.9	14.0	16.5	60	65
	H-55A	3.60(1.12)	11.3	54.5	21.3	690	10.4	25.4	55.9	8.3	—	83	87
	H-55T	4.90(1.10)	12.8	59.4	23.6	1420	18.1	30.2	47.0	4.6	—	88	91
	H-66A	2.10(1.10)	18.0	70.9	35.3	390	1.1	2.6	34.7	49.9	11.7	34	51
	H-66T	2.84(1.12)	17.4	65.7	33.3	670	2.7	13.0	50.7	27.3	6.3	55	65
	H-36	3.78(1.08)	18.2	63.4	36.6	1300	20.6	11.4	23.7	27.8	16.5	24	46
	H-50A	5.89(1.07)	13.9	40.7	26.7	2310	13.0	26.5	37.1	7.6	15.8	47	83
	H-50T	7.90(1.07)	13.8	45.1	29.4	4580	28.1	35.9	≥28.7	≤0.3	7.0	73	≥99
	H-56A	4.79(1.14)	17.1	56.6	36.9	2120	12.3	34.5	34.6	10.9	7.8	80	80
	H-56T	7.16(1.11)	16.2	52.9	35.2	4510	18.5	41.2	35.2	1.1	4.0	94	94
	H-19	4.64(1.14)	16.0	66.4	36.0	1940	→	(55.0)†	24.6	9.6	1.0	62	72
	H-21	4.82(1.12)	19.4	86.2	63.8	3700	→	(84.7)†	11.6	2.9	0.75	70	80
	H-27A	2.36(1.08)	23.8	79.2	48.6	678	3.8	14.2	28.6	42.8	10.6	17	40
	H-27T	3.77(1.09)	18.9	68.1	37.5	1330	6.3	18.5	51.2	16.2	7.8	39	76
	H-34	6.76(1.06)	21.5	78.4	43.7	5000	29.3	48.6	17.5	1.9	2.7	84	90
	H-4	2.91(1.12)	12.4	—	—	550*	11.3	2.7	32.8	49.3	3.7	25	40
	H-7	5.05(1.09)	17.8	—	—	2300*	40.8	40.8	11.2	4.8	2.4	55	70
	H-60A	4.05(1.11)	12.1	86.7	29.3	1200	22.4	35.6	30.2	6.2	5.6	83	83
	H-60T	5.15(1.10)	14.2	92.0	31.8	2110	28.2	95.2	22.1	2.7	1.8	89	89
	H-54A	3.80(1.14)	11.0	40.5	23.8	860	3.8	49.9	33.1	9.9	3.3	71	77
	H-54T	5.04(1.10)	12.7	47.4	26.2	1660	9.5	64.5	20.8	1.8	3.4	85	92
	H-24	3.76(1.11)	7.2	32.1	20.7	730	→	(20.8)†	46.7	8.2	26.3	85	85
	H-40A	3.56(1.05)	12.6	50.3	34.4	1080	4.1	71.1	21.3	2.6	0.9	85	89
	H-40T	4.86(1.04)	10.6	55.0	30.0	1770	6.7	73.7	17.1	0.5	2.0	96	97
	H-49A	1.82(1.14)	11.2	62.7	27.3	225	1.1	19.9	32.0	32.0	15.0	50	50
	H-49T	2.42(1.11)	13.8	69.7	30.5	445	0.9	29.5	41.0	19.3	9.3	68	68

1185332

TABLE III (CONTINUED)

Test Inhalation Data Summary—Mouth Breathing

Subject	Test	Particle Size. d_m (σ_g)	Min. Volume (liters)	Inspiratory Flow (lpm) Q_p[a]	Q_a[b]	$\rho d^2{}_m Q_a$	Regional Deposition % of Inhaled Aerosol Mouth	P-L[c]	T-B[d]	Alv.[e]	Exhaled Aerosol (%)	Lung Clearance (%) 10 hr	24 hr
[redacted]	H-62A	4.12(1.09)	15.9	56.4	32.6	1380	22.9	41.4	24.0	6.8	4.9	69	78
	H-62T	5.08(1.06)	17.7	69.0	36.2	2340	52.1	24.7	17.2	2.6	3.4	94	87
	H-61T	5.48(1.07)	13.9	66.8	26.9	2020	6.2	44.9	46.9	2.0	—	95	96
	H-31A	3.76(1.08)	14.6	82.0	30.1	1060	11.0	46.7	23.1	7.2	8.2	77	79
	H-31T	5.02(1.05)	12.9	74.2	30.4	1920	14.5	48.1	28.2	3.5	5.7	89	89
	H-52A	3.63(1.11)	20.4	67.4	37.2	1225	10.0	28.7	29.4	19.6	10.3	51	60
	H-52T	4.95(1.10)	(25.1)	64.9	(48.0)	(2940)	11.8	38.9	42.9	5.9	0.5	80	88
	H-29A	3.66(1.08)	15.6	67.3	34.0	1140	4.2	40.7	39.3	9.8	6.0	80	—
	H-29T	4.99(1.08)	19.6	76.1	42.6	2650	31.1	43.3	20.0	2.9	2.7	83	—
	H-37	2.34(1.06)	16.8	88.3	32.9	450	0.8	0.5	16.8	56.1	25.8	21	23
	H-47A	3.22(1.08)	15.9	56.1	30.4	790	3.5	29.2	28.3	18.1	20.9	53	61
	H-47T	7.08(1.07)	16.2	55.2	30.0	3750	41.8	33.4	16.6	0.9	7.3	80	95
	H-51A	3.52(1.11)	21.7	73.4	39.4	1220	18.7	35.7	28.8	9.6	7.2	65	75
	H-51T	4.85(1.10)	20.3	65.2	40.8	2400	33.4	40.2	20.5	2.3	3.6	86	90
	H-64A	4.04(1.07)	18.8	79.3	40.9	1660	10.2	52.8	25.6	8.1	3.4	72	76
	H-64T	5.30(1.07)	14.1	66.3	28.4	2000	14.0	65.3	15.5	2.3	2.9	85	87
	H-16	5.20(1.10)	15.0	—	—	2020*	18.6	36.6	35.2	3.9	5.7	90	90
	H-12	4.80(1.09)	17.5	—	—	2010*	56.8	22.7	16.0	0.8	3.7	92	95
	H-14	5.20(1.14)	13.5	—	—	1820*	29.6	15.3	42.2	7.4	5.5	85	85
	H-9	5.30(1.11)	14.0	—	—	1960*	27.3	36.2	25.4	2.8	8.3	80	90
	H-17	5.30(1.09)	13.5	—	—	1890*	33.3	42.2	19.0	1.0	4.5	95	95
	H-10	5.10(1.07)	19.8	—	—	2580*	43.6	18.4	28.6	6.2	3.2	82	82
	H-11	4.90(1.10)	11.7	—	—	1400*	42.0	7.8	37.0	6.5	6.7	80	85
	H-6	4.80(1.11)	16.3	—	—	1870*	32.6	2.0	57.2	3.0	5.2	85	95
	H-15	5.20(1.09)	16.0	—	—	2160*	52.0	20.1	25.1	0	2.8	92	100

* Based on Q_a equal to 2 times minute volume.

† Includes mouth deposit.

[a] Q_p = average value of peak flow in each inspiration.

[b] Q_a = average flow during inspiration.

[c] P-L = pharynx plus larynx.

[d] T-B = tracheobronchial region.

[e] Alv. = alveolar region.

at the time of the abdominal measurement. In view of the limited accuracy of the abdominal measurements, the agreement is reasonable. Better abdominal burden estimates would require a particle swallow experiment on each inhalation subject.

While deposition within the mouth did not vary greatly from subject to subject, the P-L region deposition showed marked intersubject differences. Figure 9 shows the effect of particle size on the overall head deposition for the current test series data. The data were plotted in terms of the product $\rho d^2{}_m Q_a$, since impaction was the dominant deposition mechanism in the head, and this combination of variables determines impaction efficiency in a given physical system. Thus, the variations in respiratory flow indicated in Table III were normalized, and the effect of particle size on head deposition could more readily be determined.

Figure 9 indicates that there was a large variation in impaction efficiency among the test group at a given $\rho d^2{}_m Q_a$, and that most of this variation was due to intersubject differences. Those subjects with four or more valid tests are shown by separate symbols. Calculated regression lines for each individual subject have slopes which are not significantly different at the 5% level from one another or from the slope of the line calculated for all of the data combined. Subjects [redacted] and [redacted] were at the extremes of the group, with 50% intercepts at $\rho d^2{}_m Q_a$ = 700 and 2800, respectively. In these experiments large variations in mouth deposition were observed when the type of mouthpiece was changed. In the earlier test series (H-1 through H-17),

1185333

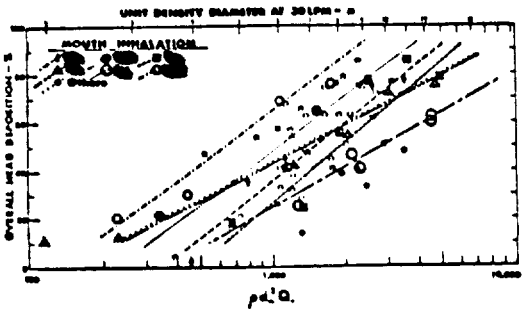

FIGURE 9. Effect of particle size on overall head deposition in mouth breathing experiments.

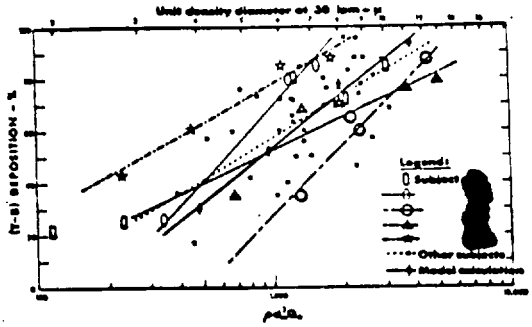

FIGURE 10. Effect of particle size on tracheobronchial (T-B) deposition. The model points were derived from the calculation described in Appendix I.

the fraction of the head deposition in the mouth averaged 64% with a range of 33% to 94%, as compared to the range of 5% to 40% in the subsequent tests. In the earlier series, the teeth clamped on tabs at the center line of the mouthpiece, restricting the cross section of the opening. In the later tests, the teeth and lips closed around the rim of the mouthpiece, leaving a wider opening.

The tracheobronchial (T-B) deposition for particles entering the trachea in the experimental inhalation tests is shown as a function of $\rho d^2{}_m Q_a$ in Figure 10. The solid diamond symbols on Figure 10 which lie close to the average of the experimental data are points from the model calculation of Appendix I, which is discussed in the next section.

The plot of (T-B) deposition on Figure 10 is similar in many respects to the head deposition plot on Fig. 9. In the (T-B) compartment, as in the head, there was a large variation in deposition at a given $\rho d^2{}_m Q_a$, with most of the variation due to intersubject differences. Also, the five subjects indicated by separate symbols show about the same relative locations on the two plots when compared to each other and to the group as a whole.

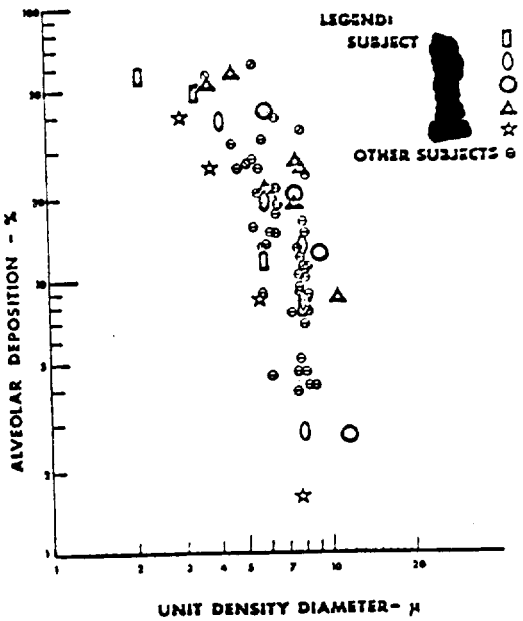

FIGURE 11. Effect of particle size on alveolar deposition.

The alveolar deposition for particles entering the trachea in the experimental inhalation tests is shown as a function of unit density diameter in Figure 11. There was a large variation in alveolar deposition among the test group at a given particle size, with most of the variation being due to intersubject differences. There was also a very marked decrease in alveolar deposition with size for particles larger than 4-micron unit density.

Discussion

Bronchial clearance has been shown to take place, and to be essentially complete, within the first postexposure day. An assumption is made that bronchial clearance is equivalent to tracheobronchial deposition, providing the basis for distinguishing between tracheobronchial and alveolar deposition. Even if some of the bronchial clearance included particles deposited in the alveolar

1185334

TABLE IV
Estimates of Activity Cleared to Abdomen

Subject	Height (inches)	Weight (pounds)	Test	Abdominal Burden Estimates: Time (hours)	Measured Activity in Abdomen, (nCi)	Head and Lung Clearence to Abdomen, (nCi)	Ratio: Measured / Clearance
[redacted]	75	250	H-32A	1.1	43.4	32.4	1.3
			H-32T	1.1	69.2	73.9	0.94
			H-41A	1.6	29.9	41.8	0.72
			H-41T	1.6	172	337	0.51
			H-48A	3.7	63.4	71.9	0.88
			H-48T	3.7	759	1208	0.63
[redacted]	70	155	H-26	1.0	146	83.1	1.8
			H-33	1.5	43.5	25.2	1.7
			H-44A	1.5	61.6	45.6	1.4
			H-44T	1.5	291	402	0.72
[redacted]	79	220	H-50A	2.9	39.7	35.2	1.1
			H-50A	23.0	62.7	50.1	1.3
			H-50T	2.9	213	264	0.81
			H-50T	23.0	304	287	1.1
[redacted]	70	175	H-25	0.8	190	184	1.0
			H-34	0.9	381	499	0.76
			H-34	3.6	555	590	0.94
[redacted]	69	167	H-40A	2.3	89.5	82.7	1.1
			H-40T	2.3	1500	1742	0.86
			H-49A	4.3	97.5	96.1	1.0
			H-49T	4.3	1449	1323	1.1
[redacted]	70	248	H-29T	1.3	744	935	0.80
			H-29T	2.3	894	1017	0.88
			H-37	2.6	28.1	31.1	0.90
			H-47A	2.0	63.8	58.4	1.1
			H-47T	2.0	150	113	1.3

region and carried to the bronchial tree by phagocytes, or if some of the bronchial deposit was not cleared within the first day, the assumption could still have a practical justification.

An important application of these data will most likely be for the calculation of the toxic dose potential of airborne contaminants. Since dose is determined by the product of the mass or number of the toxic particles and their residence time at the site of toxic action, these data provide precisely the kind of information needed for dosimetric calculations. Thus, they would provide regional deposition data in functional terms, if not necessarily in anatomic terms.

The overall head deposition data are insufficient to indicate the exact form of the relation between $\rho d^2{}_m Q_a$ and impaction efficiency. Sigmoid curves of the type obtained with inertial particle separators may be at least as valid as the straight-line plots on Figure 9. In any case, both the individual subject and the collective data show that deposition increases with increasing $\rho d^2{}_m Q_a$. The cutoff is not a sharp one; that is, the slope of the curve at the 50% intercept is low.

Parallel lines with different intercepts would be expected if the differences in deposition were largely due to differences in the air-path dimensions. Such a range of variation could have occurred as a result of differences in the oral air-path. The differences in mouth deposition produced by changing the mouthpiece configuration amply demonstrate the importance of air-path cross section.

In the case of tracheobronchial deposition, plotting the data in terms of the impaction parameter $\rho d^2{}_m Q_a$ requires some justification, since deposition due to sedimentation would be expected in the smaller ciliated airways. Partial justification is provided in Appendix I, which outlines the results of a model calcu-

1185335

lation for tracheobronchial deposition based on Weibel's[12] lung dimensions and Landahl's[3] deposition equations. It is shown that impaction would be expected to be the dominant mechanism for T-B deposition, at least for unit density diameter ≥ 4 microns, which would include all but two of the tests described in this paper.

It was previously noted that the subjects having the most efficient head collection also had the highest (T-B) removal. The reasons for this consistency are unknown. Perhaps the caliber of the oral airway is maintained sufficiently large so that the bronchial airway resistance is always controlling, in effect maintaining, a consistent cross-section progression back to the oral cavity.

In any case, the 50% intercepts range from $\rho d^2{}_m Q_a = 300$ for subject [redacted] to 1750 for subject [redacted] If we assume that there is an orderly progression of decreasing airway diameters with airway generation, as in the Weibel[12] lung model, then these data, together with the relation developed in Appendix I, indicate that subject [redacted] has airways 22% larger in diameter than the Weibel lung and that subject [redacted] has airways 31% smaller in diameter than the Weibel lung.

For a given subject, some variation in regional deposition from test to test may have resulted from variations in average airway diameters, especially those beyond the first few generations. The airways are not tubes of constant cross sections. Their diameters vary with the degree of lung inflation, which was neither measured nor controlled in these experiments.

Data on the normal variability of airway diameter are scanty. *In vivo* stereoscopic radiographic measurements of the width of the trachea and major bronchi were reported by Brückner[13] in 1952 on a group of 23 men, ages 19 to 25, and three women, ages 19 to 22. Brückner's data are presented in Table V. It can be seen that the variability in the size of the major airways in his group are similar percentagewise ($\sim\pm 25\%$) to the range inferred from the tracheobronchial deposition data in this study. The size range for the trachea and major bronchi has been measured by a number of other investigators using a variety of techniques. The techniques used and the size ranges found are given in Table V. In these data, the measurement procedure may have influenced the airway diameters measured. Also, the state of chest expansion may have varied. In any case, in most of the studies there were large variations in airway size within the test groups.

Brückner[13] also indicated that in his group the airway dimensions did not correlate well with the subject's size. His male subjects ranged in height from 165 to 186 cm (65 to 73 inches). One 184-cm male had a 16-mm trachea, while a 168-cm male had a 19-mm trachea. The smallest trachea, 15 mm on inhalation and 13 mm on exhalation, was seen on a 20-year-old 174-cm male. Thorax size did not correlate with airway dimensions either. One subject with a 100-cm chest had a 16-mm trachea, while another with an 86-cm chest had a 20-mm trachea.

In these experiments also, there was no apparent correlation between airway caliber and subject size. While subject [redacted], who had the largest indicated airway dimensions, was the largest subject (100 kg and 200 cm) in the group, there was no consistent correlation between body size and T-B deposition efficiency.

Other factors beside the caliber of the airways which would affect impaction in the tracheobronchial region are the possible curvature and irregularities in diameter within a given airway and the variation in branching angle. Brückner describes six characteristic shapes for the trachea as seen in his subjects. He describes them as: (1) cylindrical, (2) scalpel, (3) fish, (4) string of beads, (5) sugar loaf, and (6) S-form. Since diameter varied along the length, he standardized his measurement location at midway between the vocal cord and the bifurcation. For the major bronchi, the measurements were made 1 cm distal to the tracheal bifurcation.

Data on branching angles for the tracheal bifurcation are summarized in Table V. The range in each group is large, and the average values differ considerably, possibly owing to ethnic differences.

1185336

TABLE V
Airway Measurements of Various Investigators

Author and Technique	Range and (Average) of Tracheal Diameter (mm)		Range and (Average) of Major Bronchial Diameter (mm)				Range and (Average) of Bifurcation Angle	
			Right		Left			
	Men	Women	Men	Women	Men	Women	Men	Women
Brückner (1952)[18]—stereoscopic Radiography (23 men, 3 women)	15–20 (18.2) I[a] 13–20 (16.9) E[b]	14.2–15.9 (14.7) 13.5–14.6 (14.3)	14–20 (17.0) 11–18 (14.2)	11–18 (13.7) 11–16 (12.3)	10–16 (13) 8–15 (11)	9–13 (10.7) 9–12 (10.0)	64–90° (80°) 60–100° (87°)	(c) (c)
Wild (1905)[a]—tracheoscopy	16–22.5	13–16	—	—	—	—	—	—
Oppikofer (1912)[a]—paraffin-wax cast	13–25	11–18	—	—	—	—	—	—
Brüninga (1910)[a]—laryngo-bronchoscopy	15–22	13–18	12–16	10–15	10–14	9–13	—	—
Huizinga (1937)[a]—contrast-filled x-ray	15.5–18	14.8–16.9	13–16.5	13.2–14.7	12–13.8	11.5–13.5	—	—
Weingaertner (1920)[24]—radiography (9 men, 11 women)	—	—	—	—	—	—	52–88 (72°) I[a] 50–84° (65°) E[b]	60–100° (76°) 60–100° (70°)
Wang and Tai (1965)[18]—measurements on cadavers (127 male, 14 female)	9.5–22.0 (16.5) T[d] 8.0–22.5 (15.0) S[e]	9.5–16.2 (13.6) 10.5–16.5 (12.6)	9.0–21.0 (15.1) 5.0–16.0 (11.4)	10.0–20.0 (13.1) 7.0–19.0 (9.3)	7.0–17.0 (11.2) 5.0–15.0 (9.3)	7.0–13.0 (9.3) 6.0– 9.0 (7.3)	35–92° (67.6°)	55–90° (72.3°)
Kher and Makheni (1960)[18]—bronchogram (53 adults, sex not stated)	—	—	—	—	—	—	30–105° (61°)	—

[a] After Brückner.[18]
[a] Inspiration (expanded chest).
[b] Expiration.
[c] Included in data for men.
[d] Transverse.
[e] Sagittal.

In the deposition calculations in Appendix I, the angle θ between each parent and daughter tube was assumed to be 30°. Thus, the angle between the two daughter tubes would be 60°. At a constant impaction parameter or collection efficiency, the product $\rho d^2 Q$ would therefore vary inversely with sine θ. Thus if $2\theta = 35°$ instead of 60°, $\rho d^2 Q$ *would* have to be 67% higher to produce the same impaction efficiency, and if $2\theta = 100°$, it would have to be 53% lower.

Variations in branching angles at more distal generations may not affect the deposition pattern as much as at the tracheal bifurcation, since the increasing number of tubes per generation would tend to make the average angle at that generation more uniform.

A comparison of the head and tracheobronchial deposition data shows that the tracheobronchial region was a more efficient particle collector than the head in these tests. For the head, the calculated regression line for the group as a whole indicated 50% removal at $\rho d^2{}_m Q_a = 1390$, equivalent to a unit density diameter at 30 liters/min of 6.8-microns. For the T-B region, the corresponding 50% intercept was at $\rho d^2{}_m Q_a = 570$, equivalent to a unit density size at 30 liters/min of 4.4-microns.

Thus, when mouth breathing, or at least when breathing with a relatively open mouth as in these tests, the tracheobronchial tree was a significant barrier to alveolar deposition. At the same time, large particles impacting on the tracheobronchial bifurcations may be highly significant toxicologically because of their concentration on limited areas of the bronchial epithelium.

Based on physical considerations and the

1185337

work of other investigators, there is a size for maximum alveolar deposition. As discussed previously, Brown *et al.*[4] estimated this size as 1.6-microns from nose breathing experiments, while Altshuler *et al*[5] indicated that the size was greater than 2-microns, based on analysis of mouth breathing data. The ICRP Subcommittee II Task Group on Lung Dynamics[17] predicts sizes for maximal alveolar deposition in nose breathing at ~2.2, 2.0, and 1.9-microns unit density for tidal volumes of 750, 1450, and 2150 cm^3, respectively. Recalculating regional deposition from their model on the basis of air entering the trachea, the sizes for maximal alveolar deposition become ~3.5, 2.8, and 2.5-microns at 750, 1450, and 2150 cm^3, respectively.

The experimental data for particles below 4-microns are insufficient to indicate the size for maximal alveolar deposition. Additional tests with particles smaller than 4-microns are planned.

Summary

The apparatus, experimental techniques, results, and conclusions from a controlled series of particle inhalations have been described and discussed. Ninety-three aerosol inhalations were performed on 33 men and one woman using test aerosols consisting of monodisperse insoluble iron oxide spheres with ^{198}Au, ^{51}Cr, or ^{99m}Tc tags and median diameters of 1.3 to 7.9-microns (2.1 to 12.5-microns unit density). The particles were inhaled through a mouthpiece in all tests.

Measurements of the initial deposition and subsequent retention of the inhaled radioactive particles were made with an array of large scintillation detectors within a low background chamber. In 32 tests, two aerosols with different median diameters and radioactive tags were inhaled in rapid succession, simulating a simultaneous exposure. Since each tag had a different photopeak energy, the burden of each within the body could be determined from an analysis of the gamma energy spectrum.

Regional deposition was determined from the retention data. Within the lung, ciliary clearance removed particles from deposition sites along the tracheobronchial tree to the pharynx, from which they were removed to the gut by swallowing. This clearance was essentially completed within the first day, after which lung clearance proceeded at a much lower rate. The particles cleared from the lung within the first day were presumed to be the particles that deposited on the ciliated tracheobronchial tree. On this basis, the lung deposition was divided into tracheobronchial and alveolar components. The head deposition was also divided into two components. These were (1) the mouth itself and (2) the pharyngeal-laryngeal region. The deposition in the former region could be removed mechanically, while the deposition in the latter region was eventually swallowed.

For each subject tested at four or more different particle sizes, the fractional deposition in the tracheobronchial tree increased with increasing particle size. Within the alveolar region, the fractional deposition decreased with size for particles larger than 4-microns (unit density). For particles smaller than 4-microns, there was not enough experimental data to determine the size dependence. In both regions, there were large differences between individual subjects in the amount of deposition at any given particle size.

Conclusions drawn from the experimental data and analysis were as follows:

1. There are very large differences in the efficiency of the tracheobronchial tree as a particle collector among a group of 33 normal, healthy, adult human males tested.

2. In mouth breathing with an open mouth, the efficiency of the head as a particle collector approaches, but is generally lower than, the efficiency of the tracheobronchial tree.

3. Deposition of particles in the tracheobronchial tree for mouth breathing results largely from impaction, at least for particles greater than 4-microns unit density.

These experiments have generated the kind of quantitative data needed for realistic estimates of the toxic dose potential of airborne particles. However, the number and range of the variables affecting particle de-

1185338

position are so large that these data represent only a beginning in the systematic evaluation of the deposition process. Further studies to extend the particle size range downward, to characterize nasal deposition, and to study the effect of the respiratory variables are in progress.

Appendix I

Calculation of Regional Deposition in the Lung

To gain additional insight into the physical processes which interact to produce the net effects observed in the experimental phase of this study, a series of calculations were made for predicting the regional deposition within the lung for the particle size range under study.

The expected regional deposition was calculated by using impaction and sedimentation equations developed by Landahl.[3] For impaction, Landahl proposed that the fractional removal (E) at a bronchial bifurcation should be equal to:

$$E = \frac{X}{1 + X}$$

where

X = deposition parameter

$$= \frac{\rho d^2 v_{(\alpha-1)} \sin \theta}{18 \eta R}$$

where

ρ = particle density.
d = particle diameter.
$v_{(\alpha-1)}$ = air velocity in tube of generation $(\alpha-1)$.
θ = branching angle between tube α and tube $(\alpha-1)$.
η = air viscosity.
R = radius of tube of generation α.

But

$$v_{(\alpha-1)} = \frac{Q}{S_{(\alpha-1)}}$$

where

Q = flow rate.
$S_{(\alpha-1)}$ = total cross section of all tubes of generation $(\alpha-1)$

and

$$R_\alpha = \frac{D_\alpha}{2}$$

where

D_α = diameter of tube of generation α.

For $\eta = 189 \times 10^{-6}$ gm/cm-sec (for air at 37°C), Q in liters/min, d in microns, ρ in gm/cm³, D in cm, S in cm²,

$$X = 10^{-4} \frac{\rho d^2 Q \sin \theta}{D_\alpha S_{(\alpha-1)}}$$

Assuming that $\sin \theta = 0.5$ and is constant from generation to generation, we have

$$X = 5.0 \times 10^{-5} \frac{\rho d^2 Q}{D_\alpha S_{(\alpha-1)}}$$

For each branching of the bronchial tree, the fractional removal can be calculated in terms of the product $\rho d^2 Q$. This has been done using the Weibel[12] lung dimensions to obtain the product $(D_\alpha S_{(\alpha-1)})$. Calculations have been made only for deposition on inspiration. Deposition due to impaction on expiration should be relatively small in most cases for two reasons. One, within the range of particle size and breathing velocity under study, most of the inhaled aerosol will be impacted in the bronchial tree on inspiration, or deposited in the pulmonary spaces during inspiration and expiration by sedimentation, leaving relatively little that could be impacted in the larger airways on expiration. The second consideration is that the impaction efficiency for each branch point is lower on expiration than on inspiration. On expiration, the air velocity is increasing from generation to generation, with the particles tending to lag behind. Also, whereas on inspiration the particle goes from a larger to a smaller tube, on expiration the particle is entering a larger tube and must traverse a greater distance in order to impact.

For sedimentation, Landahl proposed the following expression for the fractional deposition S:

$$S = 1 - e^{(-0.8 U_t \cdot t \cdot \cos\Psi)/R}$$

where

U_t = terminal settling velocity.
t = time of travel along tube.
Ψ = angle of tube to horizontal.
R = radius of tube.

1185339

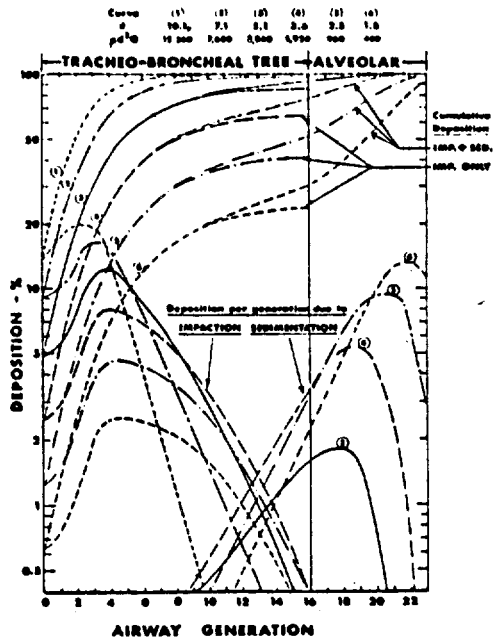

FIGURE 12. Calculated deposition in the lung at 30 liters/min.

Assuming a value of cos Ψ equal to 2/Π, and a suitable flow rate, which determines t in each generation of airway, the fractional deposition due to sedimentation in each generation of a lung with the Weibel dimensions can be calculated.

Calculations were made to determine the deposition due to the combined effects of impaction and sedimentation for six different particle sizes at a flow rate of 30 liters/min, which is close to the average inspiratory flow in the inhalation tests.

Figure 12 shows the calculated deposition during inspiration per airway generation due to both impaction and sedimentation for these conditions. It also shows the cumulative deposition due to impaction only and that due to the combined effects of impaction and sedimentation at each generation. It can be seen that, for particles larger than 2.5-microns suspended in air reaching the alveolar spaces, total deposition approaches 100% during the inspiratory phase. Sedimentation should be equally effective on expiration, so that for particles less than 2.5-microns, where deposition on inspiration is incomplete, there should be a significant increment of deposition in the finer airways on expiration.

The overall deposition within the lung due to sedimentation for these smaller particles will be influenced by the tidal volume and the duration of breath holding between inhalation and exhalation, since not all the air inhaled reaches the same depth in the lung.

Discussion of Calculated Particle Deposition in the Lung

From the curves of predicted deposition per airway generation in Figure 12, the following are the expected features of the particle deposition for particles within the size range studied.

1. Most of the deposition within the tracheobronchial tree should be due to impaction.
2. Essentially all the impaction should take place within the first ten to twelve airway generations.
3. Most of the deposition in the tracheobronchial tree beyond the twelfth generation should be due to sedimentation.
4. The fractional deposition per generation reaches a minimum in the vicinity of the twelfth generation and increases toward the end of the bronchial tree.
5. The maximum impaction deposition per generation shifts from generation two for 10.1-micron particles ($\rho d^2 Q$ = 15,360) to the vicinity of generation five for $d \leq$ 2.5-microns ($\rho d^2 Q$ = 1920).
6. In the generations where impaction is the dominant mechanism, deposition should occur primarily on the bronchial bifurcations.
7. For the larger particles, the calculation indicates that most of the deposition should occur within the first four generations. For the smaller particles, the calculated impaction deposition is spaced more uniformly along the bronchial tree.

Thus, in test runs where bronchial clearance accounts for 90% or more of the initial deposit, a very large fraction of the aerosol should impact within the first few generations.

1185340

On the other hand, for tests where there is a major fraction deposited in the alveolar region, we should expect the bronchial deposit to be spread fairly uniformly along the bronchial tree, with a larger proportion of the bronchial deposit being cleared toward the end of the bronchial clearance phase.

In the calculation of the impaction efficiency, the impaction parameter, X, was shown to be

$$X = \frac{\rho d^2 Q \sin\theta}{D_a S_{(a-1)}} \times 10^{-4}$$

$$= \frac{(X)\ (\pi/4)\ (10^4)}{\sin\theta} [D_a D_{(a-1)}^2] = kD_a D_{(a-1)}^2$$

Thus:

$$\rho d^2 Q = \frac{(X)\ (D_a S_{(a-1)})}{\sin\theta} \times 10^4$$

$$= \frac{(X)\ (D_a)\ (\pi/4\ D_{(a-1)}^2)}{\sin\theta} \times 10^4$$

If there is an orderly progression of airway diameters, then $\rho d^2 Q$ would vary as the third power of the airway diameter at any given level. As a result, at the same collection efficiency, a 26% difference in airway diameter would cause a 100% difference in the product $\rho d^2 Q$.

Acknowledgments

Grateful appreciation is due to our coworkers on the pulmonary deposition and clearance project, especially Mr. Jack Spiegelman, Mrs. Linda (Block) Rose, Mr. Daniel Alessandro, and Dr. Carl Crawford. Their assistance in the preparation of the colloidal aerosol feed suspensions and in the collection and reduction of the voluminous experimental data was an essential aspect of the performance of this study. The assistance of Mr. Samuel Posner in the preparation of the electronmicrographs is appreciatively acknowledged.

A special word of appreciation is due our colleagues, too numerous to mention, who enthusiastically volunteered to be test inhalation subjects.

References

1. Landahl, H. D., T. N. Tragewell, and W. H. Lassen: On the Retention of Airborne Particulates in the Human Lung: II. *A.M.A. Arch. Ind. Hyg. Occup. Med. 3:* 359 (1951).
2. Landahl, H. D., T. N. Tragewell, and W. H. Lassen: Retention of Airborne Particulates in the Human Lung: III. *A.M.A. Arch. Ind. Hyg. Occup. Med. 6:* 508 (1952).
3. Landahl, H. D.: On the Removal of Airborne Droplets by the Human Respiratory Tract: I. The Lung. *Bull. Math. Biophys. 12:* 43 (1950).
4. Brown, J. H., K. M. Cook, F. G. Ney, and T. Hatch: Influence of Particle Size upon the Retention of Particulate Matter in the Human Lung. *Amer. J. Public Health 40:* 450 (1950).
5. Altshuler, B., E. D. Palmes, and N. Nelson: Regional Aerosol Deposition in the Human Respiratory Tract. In *Inhaled Particles and Vapours II.* (C. N. Davies, ed.), Pergamon Press, Oxford (1967).
6. Albert, R. E., and C. L. Arnett: Clearance of Radioactive Dust from the Human Lung. *A.M.A. Arch. Ind. Health 12:* 99 (1955).
7. Albert, R. E., H. G. Petrow, A. S. Salam, and J. R. Spiegelman: Fabrication of Monodisperse Lucite and Iron Oxide Particles with a Spinning Disc Generator. *Health Phys. 10:* 933 (1964).
8. Albert, R. E., M. Lippmann, J. Spiegelman, C. Streelow, W. Briscoe, P. Wolfson, and N. Nelson: The Clearance of Radioactive Particles from the Human Lung. In *Inhaled Particles and Vapours II* (C. N. Davies, ed.), Pergamon Press, Oxford (1967).
9. Albert, R. A., M. Lippmann, J. Spiegelman, A. Liuzzi, and N. Nelson: The Deposition and Clearance of Radioactive Particles in the Human Lung. *Arch. Environ. Health 14:* 10 (1967).
10. Lippmann, M., and R. E. Albert: A Compact Electric-Motor Driven Spinning Disc Aerosol Generator. *Amer. Ind. Hyg. Assoc. J. 28:* 501 (1967).
11. Albert R. E., and B. Altshuler: The Use of a Whole-Body Counter for Determining Pulmonary Deposition and Clearance of Inhaled Particles in Man. In *Whole-Body Counting.* International Atomic Energy Agency, Vienna (1962).
12. Weibel, E. R.: *Morphometry of the Human Lung,* Academic Press, New York (1963).
13. Brückner, H.: Die Anatomie der Luftröhre beim lebenden Menchen. *Z. Anat. Entwicklungsgeschichte 116:* 276 (1952).
14. Weingaertner, M.: Physiologie und topographische Studien am Tracheo-Bronchialbaum des lebenden Menschen. *Arch. Laryngol. Rhinol. 32:* 1 (1920).
15. Wang, K.-P., and H.-P. Tai: The Measurement of the Trachea and the Bronchi in the Adult Chinese. *Acta. Anat. Sinica 8:* 397 (1965).
16. Khera, G. A., and J. S. Makhani: A Preliminary Study of the Lengths of the Two Main Bronchi and Angle at the Carina. *J. Indian Med. Assoc. 34:* 262 (1960).
17. Report of Task Group on Lung Dynamics to ICRP Committee 2. Deposition and Retention Models for Internal Dosimetry of the Human Respiratory Tract. *Health Phys. 12:* 173 (1966).

1185341